Applied Chemical Engineering (2024) Volume 7 Issue 3
doi: 10.59429/ace.v7i3.5563

RESEARCH ARTICLE

A computational model for the dietary control of insulin, glucose, fatty acid metabolism and type 2 diabetes

Baozhu Guo, Shih-Pin Lee*

Department of Public Health, International College, Krirk University , Bang Khen, Bangkok, 10220, Thailand
***Corresponding author:** Shih-Pin Lee, cornelius.lee@gmail.com

ABSTRACT

Non-alcoholic fatty liver disease (NAFLD) is a significant global public health issue, closely related to poor dietary habits and excessive energy intake. Type 2 diabetes （T2DM） is closely related to NAFLD. Due to the complex regulation of dietary factors on the interaction between insulin, glucose, and free fatty acids (FFA), existing metabolic models have limitations in characterizing the dynamic response of this system. This paper uses an improved mathematical model to simulate the dynamic effects of different dietary compositions on insulin, glucose, and FFA, the study adopts a delayed feedback mechanism to construct a system of differential equations, which describes the relationship between postprandial insulin secretion and the fluctuations of glucose and FFA. The results show that the model can effectively simulate the fluctuating behavior of metabolic parameters under postprandial conditions, verifying its predictive potential in the study of NAFLD and dietary interventions.

Keywords: Non-alcoholic fatty liver disease; free fatty acids; Insulin; Glucose; Dietary; Type 2 diabetes.

ARTICLE INFO

Received: 13 November 2024
Accepted: 26 November 2024
Available online: 6 December 2024

1. Introduction

Non-alcoholic fatty liver disease (NAFLD) is a disease marked by the accumulation of fat within the liver. Its pathogenesis is complex, and free fatty acids (FFA) play a crucial role in it. The relationship between type 2 diabetes （T2DM） and NAFLD is complex and bidirectional[1, 2]. It is difficult to distinguish whether NAFLD plays a causal role in the development of T2DM or whether it is simply a result of T2DM[3]. High FFA levels can lead to metabolic disorders like insulin resistance and hepatocyte injury, which worsen the development of NAFLD[4, 5]. Studies have shown that NAFLD is closely related to insulin resistance, which may be the core mechanism leading to reduced insulin levels and increased FFA[6, 7]. Insulin resistance may raise FFA levels in the blood. This can lead to fat accumulation and inflammation in the liver, which may then develop into NAFLD. The lipid accumulation and inflammation in NAFLD can be aggravated, making patients with T2DM more susceptible to liver damage[6, 7].Consequently, an in-depth exploration of the association between insulin, FFA, NAFLD and T2DM is highly significant for formulating effective intervention strategies.

Exist mathematical models have been developed to simulate metabolic interactions and provide insights into the regulation of glucose, insulin, and lipid levels in response to dietary inputs.

Classical models, such as those by Sturis et al.[8]and Tolić et al.[9], have been instrumental in establishing foundational knowledge about the glucose-insulin feedback system. These models describe core mechanisms, including insulin-stimulated glucose uptake and inhibition of hepatic glucose production. However, their design often limits the exploration of lipid metabolism and postprandial FFA responses, as they focus predominantly on glucose and insulin dynamics, thus excluding important dietary influences. More recent models, König et al.[10] and Dalla et al.[11] have made significant strides by incorporating multiple compartments to reflect organ-specific metabolic functions, enabling a more realistic simulation of postprandial states. These models, however, frequently overlook the broader systemic effects of diet and the detailed interaction between FFA and glucose metabolism. Mathematical modeling has emerged as a powerful tool to understand metabolic systems by integrating biochemical interactions and simulating metabolic changes under various conditions. Models focusing on insulin-glucose dynamics[8, 9] and hepatic lipid metabolism[12] provide insight into key regulatory processes. These models help explore how diet and energy balance influence insulin sensitivity, hepatic glucose uptake, and FFA levels in the bloodstream. However, many existing models either simplify these dynamics or overlook the comprehensive effects of dietary inputs on systemic responses.

This study aims to develop a mathematical model that encapsulates the interactions between glucose, insulin, and FFA regulated by diet. Building on the glucose-insulin feedback model of Tolić et al.[9] and Pratt et al.[12] framework for hepatic lipid metabolism, this model simulates the metabolic response to mixed meals under fed and fasted states. We hypothesize that by incorporating dietary variables, this model will more accurately reflect postprandial oscillations in insulin and FFA levels and can thus serve as a predictive tool for metabolic studies, dietary intervention planning, and clinical applications.

2. Materials and methods

This model is founded on several hypotheses backed by the literature[8, 9, 12, 13]. Nevertheless, to prevent this stage of model development from becoming too onerous, some details of the process are omitted. Sturis and Tolić [8, 9] proposes a systematic insulin -glucose model which served as a basis for the glucose and insulin equations. Similarly, Pratt and Kosic [12, 13] described the (fasting) FFA kinetics are described by kinetic equations. The following insulin -glucose feedback loops are included in the model: glucose stimulates pancreatic insulin secretion, insulin stimulates glucose uptake and inhibits hepatic glucose production and glucose enhances its own uptake. The system contains two significant delays. One delay is related to the fact that the physiological action of insulin on the utilization of glucose is correlated with the concentration of insulin in a slowly equilibrating intercellular compartment rather than with the concentration of insulin in the plasma. The other delay is associated with the time lag between the appearance of insulin in the plasma and its inhibitory effect on the hepatic glucose production. The insulin-glucose model has three main variables: the amount of glucose in the plasma and intercellular space, G, the amount of insulin in the plasma, I_p , and the amount of insulin in the intercellular space, I_i . In addition, there are three variables, x_1 , x_2 , and x_3 , that represent the above-mentioned delay between insulin in plasma and its effect on the hepatic glucose production. V_p is the distribution volume for insulin in plasma, and V_i the effective volume of the intercellular space. Insulin degradation is assumed to be exponential, with time constant t_p for insulin in plasma and ti for insulin in the intercellular space. Assume that the delay is of third order and the total time is t_d . G_{in} with the glucose infusion rate of 216 mg min^{-1} . Hepatic glucose ,G_L; Hepatic glycogen , Y_L; Hepatic-6-phospahte , P_L; Free fatty acids in liver ,R_L; Triacylglycerol storage pool in liver, A_L; TAG storage pool T_L; TAG secretary pool in liver ,S_L; Adipose glycerol, L_A; Muscle pyruvate ,R_m; Plasma exogenous CM TAG ,T_{CB}; Plasma endogenous LP TAG ,T_{LB}. The overall scheme of reactions and transport is illustrated in **Figure 1.**

The models were represented in SBML[14], which is a standard for biochemical networks, using the Python tool SBML shorthand[15]. Model diagrams were constructed in CellDesigner[16]in accordance with the Systems Biology Graphical Notation (SBGN)[17]. The SBML code was deposited in the Biomodels database and assigned the identifier BIOMD0000000372[9] and BIOMD0000000382[8],but Pratt's model[12] and Kosic's model[13]not in BioModels, so we reconstruct this model through the details of the paper and omit the unnecessary parts, such as muscle, adipose tissue.

In this paper, an analysis of the mathematical model of hepatic lipid metabolism was carried out. The model in the form of 18 differential kinetic equations (Supplementary Material **Table 1**) including 64 parameters (Supplementary Material **Table 2**) describes the metabolic response of the organism to meals with different proportions of macronutrients with a special emphasis on FFA. Pratt et al.[12] propose the macronutrient metabolism pathway. The model includes three compartments: liver, blood plasma and pancreas.

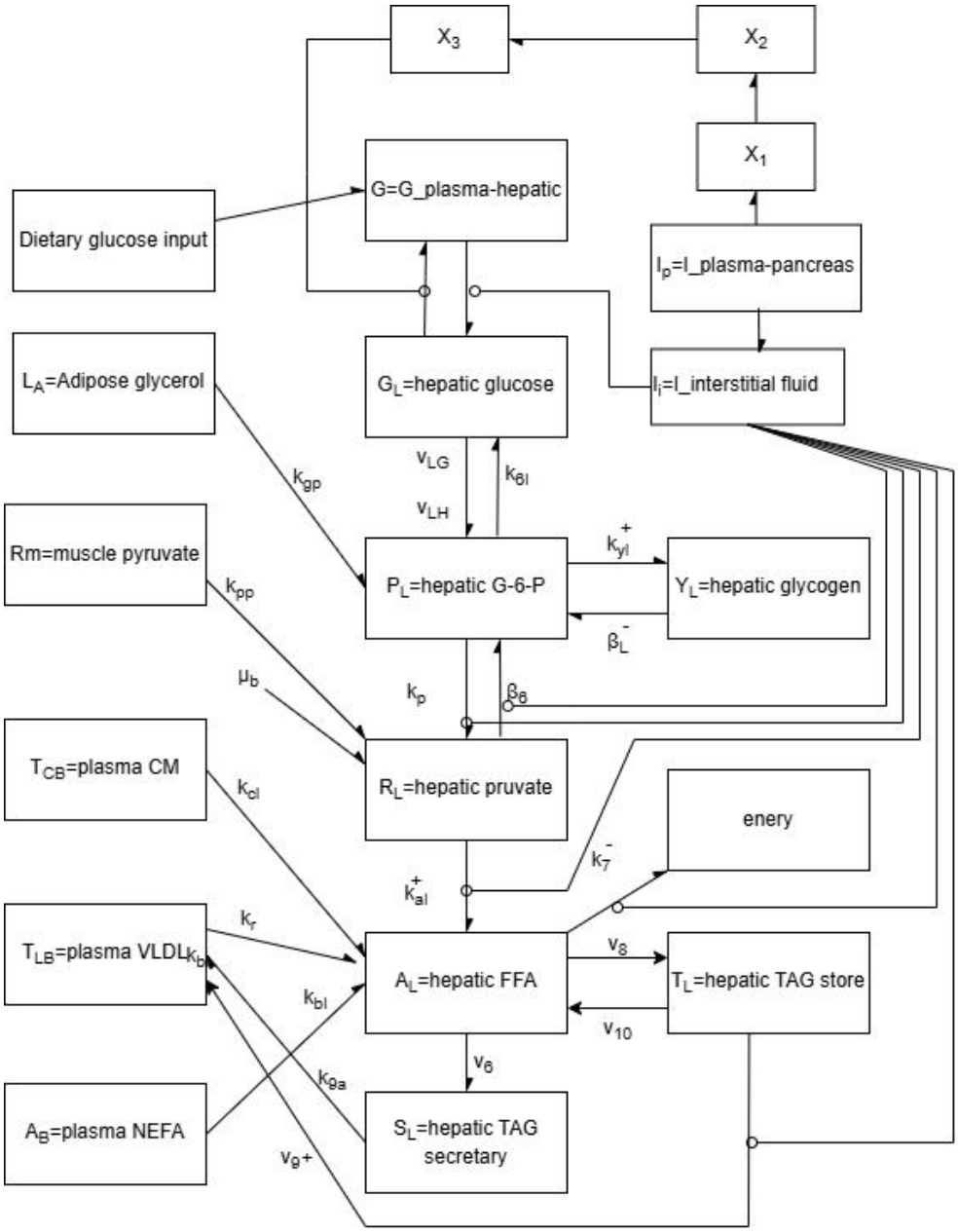

Figure 1. Dietary control of insulin, glucose, and fatty acid model[8, 9, 12]

Model diagram: at the top we show dietary input of glucose, on the right and center are hepatic components, on the upper right are pancreas , on the left are plasma compartments, In addition to the variable names and descriptions, we include a parameter associated with each flux, plus and minus superscripts represent insulin stimulated and insulin inhibited pathways (A description of each species is in the supplement).

3. Results

3.1. Simulation of insulin and hepatic glucose level in normal condition

The oscillation amplitude of insulin secretion increased with the increase of glucose infusion rate, which was divided into two parts, one was intravenous injection, the other was oral glucose absorption, and the total absorbed glucose was 214.6 mg min^{-1}. When the oral glucose is set at 115.28 mg min^{-1} and the intravenous infusion is set at 99.32 mg min^{-1}, if the intravenous and oral glucose are continuously given, hepatic glucose and insulin show periodic oscillations. (**Figure 2**)

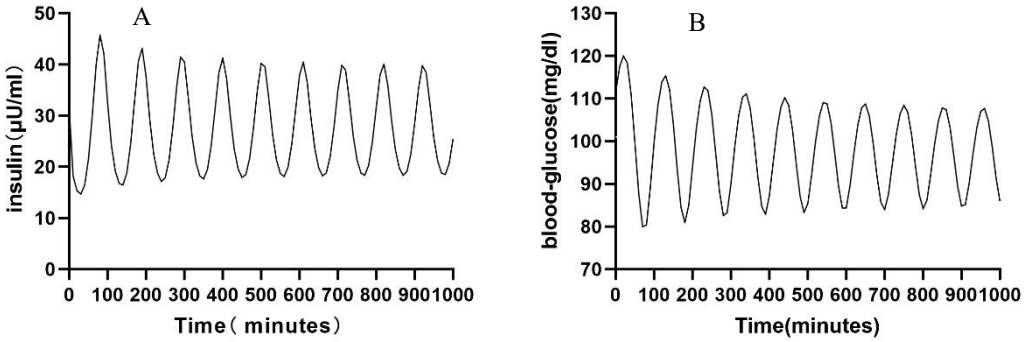

Figure 2. The time evolution of the insulin (A)and blood glucose (B)concentration.

3.2. Hepatic glycogen, insulin, plasma glucose and FFA at different diet intake

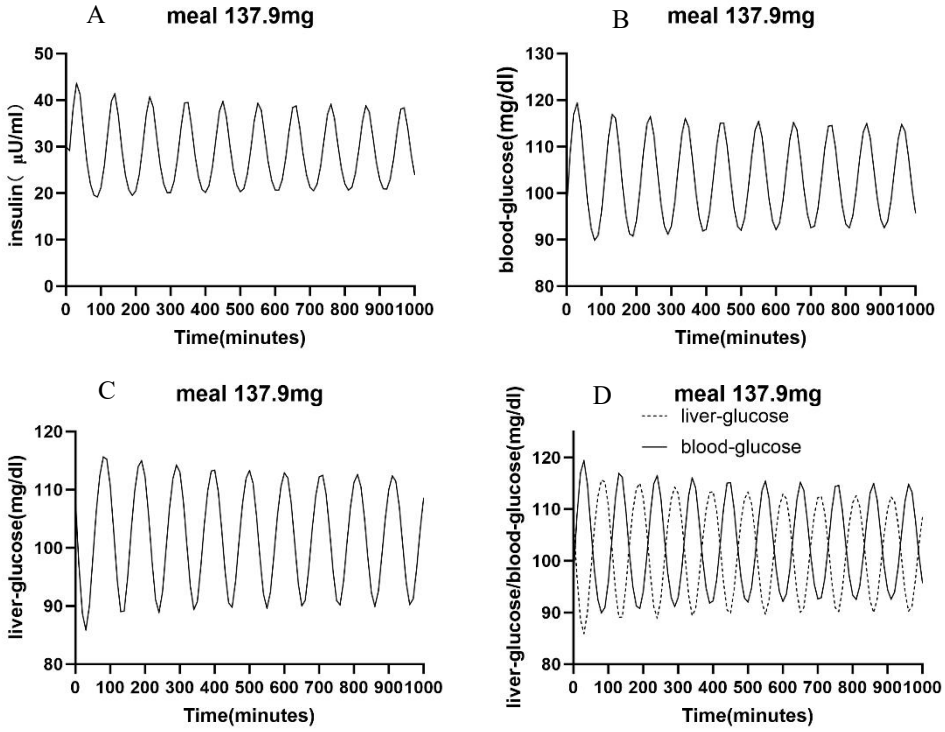

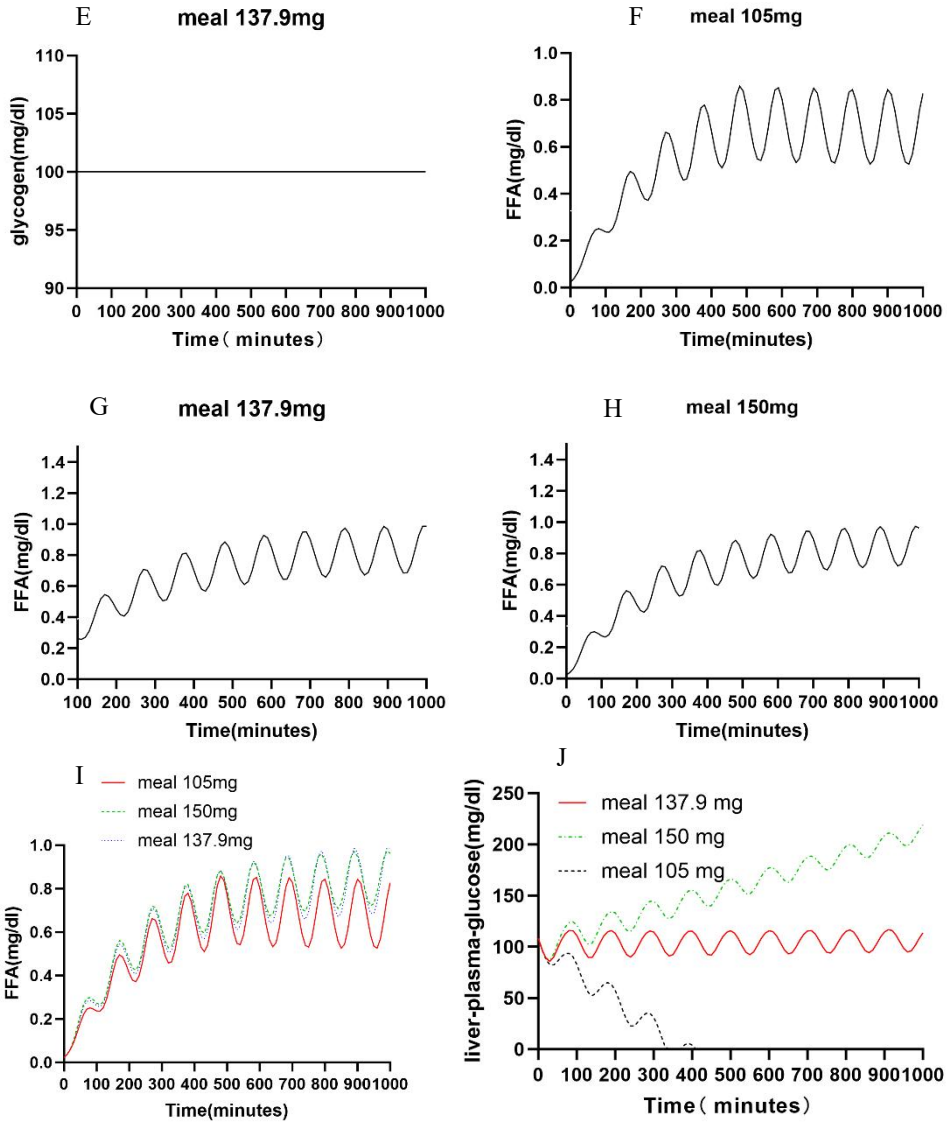

Figure 3. A predictive model of hepatic glycogen, insulin, glucose and FFA metabolism.

Compared with **Figure 3** (A,B) and **Figure 2** (A,B), the amplitude of insulin and blood glucose did not change substantially, indicating that the fitting of the two models did not affect the original model. When the intake was 137.9 mg glucose(higher than the equilibrium value of the model alone), (**Figure 3**A)Liver plasma insulin feedback , (**Figure 3**B) glucose in blood and (**Figure 3**C) the glucose in liver changed. Simultaneous contrast of hepatic glucose and blood glucose (**Figure 3**D); Changes in hepatic glycogen (**Figure 3**E). The changes of FFA when the intake was 105 mg (**Figure 3**F), 137.9 mg (**Figure 3**G), and 150mg (**Figure 3**H) respectively. (**Figure 3**I) Simultaneous comparison of fatty acid changes when meal intake was 105 mg(red line), 137.9 mg(blue dashes) and 150 mg (green dashes), respectively. (**Figure 3**J) Simultaneous comparison of liver plasma glucose changes when meal intake was 105 mg (black line), 137.9 mg (red line) and 150 mg (green dashes), respectively

Figure 3B shows that when the food intake is 137.9 mg containing glucose, liver blood glucose fluctuates between 120-80 mg, which is consistent with the physiological phenomenon of mammals. **Figure 3**C shows that hepatic glucose also fluctuates between 120 mg-80 mg. In **Figure 3**D, glucose in the blood and glucose in the liver oscillate opposite, that is, glucose in the blood is at the highest amplitude, but glucose in the liver is at the trough; In contrast, while glucose in the blood troughs, glucose in the liver peaks and oscillates consistently with each other. In **Figure 3**E, the hepatic glycogen content remained constant at 100 g, neither increasing nor decreasing with the increase of food intake, which was consistent with

mammalian physiological phenomena. As shown in **Figure 3**F, when the food intake was 105mg and glucose content, the free fatty acids increased rapidly and maintained a fixed level of oscillation; When the food intake increased to 137.9 mg (**Figure 3**G), the FFA also increased, and finally fluctuated in a fixed range. When the meal intake was increased to 150 mg (**Figure 3**H) containing glucose, the free fatty acid shock gradually disappeared. **Figure 3**I shows the simultaneous comparison of FFA content changes when the meal intake was 105 mg (low level), 137.9 mg equilibrium) and 150 mg (high-level). **Figure 3**J shows the simultaneous comparison of glucose content changes when the meal intake was 105 mg (glucose decline), 137.9 mg (glucose equilibrium) and 150 mg (glucose rise).

3.3. Simulation of insulin and FFA levels in diabetic condition

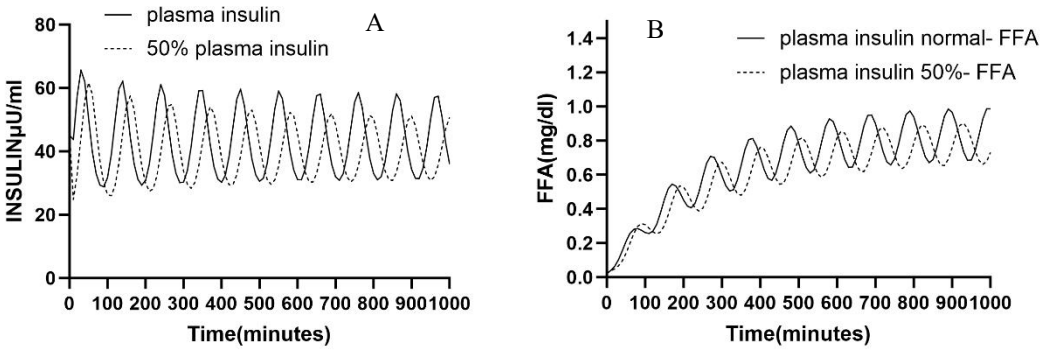

Figure 4. Simulation of normal insulin secretion and reduce secretion by 50%.

In the later stages of diabetes, insulin secretion usually decreases significantly and may be only about 50% of the level in normal healthy human[18]. In the model, we simulated 50% of normal insulin production (**Figure 4**A) and explored the relationship between insulin and FFA (**Figure 4**B). The results showed that when insulin production decreased, FFA production also decreased.

4. Discussion

This study model provides a simplified framework for investigating the effects of diet on postprandial blood glucose metabolism and lipid metabolism in the liver, which is suitable for the study of metabolic disorders like T2DM mellitus and NAFLD. This section will discuss the advantages and disadvantages of this model, such as the benefit of delayed insulin secretion, the lack of β-cell mass, limitations, and directions for improvement.

The design of this model offers significant application potential for metabolic studies focusing on the response of glucose and lipids to different dietary components after meals. Similar models have been applied to model the metabolic dynamics of T2DM and NAFLD, in which fluctuations in glucose and FFA play a crucial role in disease progression.[19-21]. The model is aligned with contemporary research trends by incorporating dietary responses, with an emphasis on dietary adjustments for controlling blood glucose and lipids. These applications also demonstrate the usefulness of the model in simulating the metabolic responses to different dietary components in the context of metabolic syndrome (e.g., T2DM, NAFLD, etc.), and offer insights into dietary intervention strategies for the management of metabolic syndrome. The combination of dietary input is the highlight of this model, which can simulate the postprandial response of blood glucose and hepatic glucose in both feeding and fasting states, overcoming the limitations of the model that focuses only on intravenous glucose infusion, and providing a more realistic description of glucose and lipid metabolism. However, it neglects glycogen intermediates such as glucose-1-phosphate, uridine diphosphate glucose, inorganic phosphate, and pyrophosphate, which play a vital role in the conversion between blood glucose and glycogen and have a considerable impact on metabolic pathways. Nevertheless, the model

disregards them.[22]. In addition, simplifying hepatic lipid metabolism, such as ignoring protein interactions such as skeletal muscle, adipose tissue, and plasma variables, may limit the application of this model in high-fat diet studies[5]. Another deficiency is the lack of beta cell mass production, which is not a good description of beta cell changes under hyperglycemia. Classic β cell mass model is Topp et al.[23], mild hyperglycemia has a negative feedback mechanism with β cell mass, while extreme hyperglycemia has a positive feedback mechanism with β cell mass. Another model development β cell mass model of diabetes in fa/fa rats in 2007[24], show that both excessive insulin resistance and insufficient adaptation contribute to the initiation of hyperglycemia[24]. Current models view beta cell mass as static, restricting its application in long-term metabolic studies. Not modeling the changes in beta cell populations adapting to chronic insulin needs over time can result in inaccurate predictions of persistent hyperglycemia[25]. For example, in people with long-term diabetes, beta cell mass may gradually decrease. Models that do not reflect this change will overestimate the amount of insulin secreted, resulting in inaccurate predictions of blood glucose levels.

The delayed insulin secretion is a very important feedback link in the model of insulin metabolism. If there were no delay, insulin would not oscillate. Therefore, the analysis of insulin delay is the key to accurately simulate the metabolic response. The model incorporates the insulin secretion delay, so it can capture the oscillation behavior of insulin-glucose in the feedback loop. Such as those described by recent studies[26],simulate time lags between insulin secretion and its physiological effects, crucial for maintaining metabolic stability. For instance, insulin delays allow for more precise regulation of blood glucose following dietary intake, as delayed secretion can prevent overcompensation that leads to hypoglycemia. These delays also reflect real-life physiological conditions where insulin effects on glucose metabolism are not immediate. In comparison to models without insulin secretion delays[27], such as purely linear feedback models, our model provides an advantage by offering a closer approximation of physiological insulin responses. Including delays enables simulations of postprandial glucose and FFA oscillations, reflecting the temporal dynamics essential for metabolic stability. This is particularly useful for studies focused on oscillatory regulation in metabolic systems, as disruptions in delay timings have been linked to insulin resistance and glucose intolerance[28]. The delay mechanism in this model also allows for exploring potential therapeutic approaches that target insulin secretion timing, highlighting the role of temporal regulation in managing metabolic disorders.

In the later stage of diabetes, especially in patients with type 2 diabetes, as the disease progresses, the function of β cells gradually declines and the ability to secrete insulin is significantly reduced. Studies have shown that patients with type 2 diabetes secrete 50% to 70% less insulin than normal people[29, 30], and many diabetics have insulin resistance before the insulin level is lower in the later stage[31, 32]. This resistance leads to increased release of FFA. This, in turn, leads to the accumulation of fat in the liver. For example, the liver uses excessive free fatty acids to synthesize triglycerides and store them to form fatty liver[33, 34]. In the later stages of diabetes, however, fatty liver disease can be greatly improved through weight loss promotion or the direct treatment of liver fat accumulation[35]. This model can well reproduce the corresponding changes in blood glucose, hepatic glucose and FFA when insulin secretion is reduced, which is consistent with the reality. When insulin production is 50% of normal, it can be found that blood glucose and hepatic glucose increase significantly, which affects the content of free fatty acids. Nicely reproduced that T2DM patients are more likely to develop fatty liver disease, providing insights into the relationship between T2DM and FFA.

Future studies of this model should focus on exploring the effects of glucose changes on pancreatic β cells, including their generation and death, and the effect of circadian genes on blood glucose balance and hepatic lipid metabolism. Moreover, this can be achieved by combining islet β cell mass changes, hepatic lipid metabolism intermediates, and circadian factors of fatty acid levels, like cortisol and melatonin.

5. Conclusion

In conclusion, this insulin-glucose-FFA model provides a versatile tool for exploring dietary impacts on postprandial metabolism across various scenarios. Future iterations that integrate adaptive β-cell responses and insulin secretion delays may strengthen its relevance, offering a valuable resource for both research and clinical applications in metabolic disease management.

Conflict of interest

The authors declare no conflict of interest.

References

1. Targher G, Corey KE, Byrne CD, Roden M. The complex link between NAFLD and type 2 diabetes mellitus—mechanisms and treatments. Nature reviews Gastroenterology & hepatology. 2021;18(9):599-612.
2. Cernea S, Raz I. NAFLD in type 2 diabetes mellitus: Still many challenging questions. Diabetes/Metabolism Research and Reviews. 2021;37(2):e3386.
3. Valenti L, Bugianesi E, Pajvani U, Targher G. Nonalcoholic fatty liver disease: cause or consequence of type 2 diabetes? Liver International. 2016;36(11):1563-79.
4. Tilg H, Moschen AR. Evolution of inflammation in nonalcoholic fatty liver disease: the multiple parallel hits hypothesis. Hepatology. 2010;52(5):1836-46.
5. Perry RJ, Peng L, Barry NA, Cline GW, Zhang D, Cardone RL, et al. Acetate mediates a microbiome-brain-beta-cell axis to promote metabolic syndrome. Nature. 2016;534(7606):213-7.
6. Deng M, Wen Y, Yan J, Fan Y, Wang Z, Zhang R, et al. Comparative effectiveness of multiple different treatment regimens for nonalcoholic fatty liver disease with type 2 diabetes mellitus: a systematic review and Bayesian network meta-analysis of randomised controlled trials. BMC medicine. 2023;21(1):447.
7. Mu W, Cheng X-f, Liu Y, Lv Q-z, Liu G-l, Zhang J-g, et al. Potential nexus of non-alcoholic fatty liver disease and type 2 diabetes mellitus: insulin resistance between hepatic and peripheral tissues. Frontiers in pharmacology. 2019;9:1566.
8. Sturis J, Polonsky KS, Mosekilde E, Van Cauter E. Computer model for mechanisms underlying ultradian oscillations of insulin and glucose. American Journal of Physiology-Endocrinology And Metabolism. 1991;260(5):E801-E9.
9. Tolić IM, Mosekilde E, Sturis J. Modeling the insulin–glucose feedback system: the significance of pulsatile insulin secretion. Journal of theoretical biology. 2000;207(3):361-75.
10. König M, Bulik S, Holzhütter HG. Quantifying the contribution of the liver to glucose homeostasis: a detailed kinetic model of human hepatic glucose metabolism. PLoS computational biology. 2012;8(6):e1002577.
11. Dalla Man C, Rizza RA, Cobelli C. Meal simulation model of the glucose-insulin system. IEEE Trans Biomed Eng. 2007;54(10):1740-9.
12. Pratt AC, Wattis JA, Salter AM. Mathematical modelling of hepatic lipid metabolism. Math Biosci. 2015;262:167-81.
13. Kosic M, Benkovic M, Jurina T, Valinger D, Gajdos Kljusuric J, Tusek AJ. Analysis of Hepatic Lipid Metabolism Model: Simulation and Non-Stationary Global Sensitivity Analysis. Nutrients. 2022;14(23).
14. Hucka M, Finney A, Sauro HM, Bolouri H, Doyle JC, Kitano H, et al. The systems biology markup language (SBML): a medium for representation and exchange of biochemical network models. Bioinformatics. 2003;19(4):524-31.
15. Wilkinson DJ. Stochastic modelling for systems biology: Chapman and Hall/CRC; 2018.
16. Funahashi A, Matsuoka Y, Jouraku A, Morohashi M, Kikuchi N, Kitano H. CellDesigner 3.5: a versatile modeling tool for biochemical networks. Proceedings of the IEEE. 2008;96(8):1254-65.
17. Novère NL, Hucka M, Mi H, Moodie S, Schreiber F, Sorokin A, et al. The systems biology graphical notation. Nature biotechnology. 2009;27(8):735-41.
18. Finck BN. Targeting metabolism, insulin resistance, and diabetes to treat nonalcoholic steatohepatitis. Diabetes. 2018;67(12):2485-93.
19. Stefanovski D, Punjabi NM, Boston RC, Watanabe RM. Insulin Action, Glucose Homeostasis and Free Fatty Acid Metabolism: Insights From a Novel Model. Frontiers in endocrinology. 2021;12:625701.
20. Li Y, Chow CC, Courville AB, Sumner AE, Periwal V. Modeling glucose and free fatty acid kinetics in glucose and meal tolerance test. Theor Biol Med Model. 2016;13:8.

21. Roy A, Parker RS. Dynamic modeling of free fatty acid, glucose, and insulin: An extended" minimal model". Diabetes technology & therapeutics. 2006;8(6):617-26.
22. Petäjä EM, Yki-Järvinen H. Definitions of normal liver fat and the association of insulin sensitivity with acquired and genetic NAFLD—a systematic review. International journal of molecular sciences. 2016;17(5):633.
23. Topp B, Promislow K, deVries G, Miura RM, Finegood DT. A model of beta-cell mass, insulin, and glucose kinetics: pathways to diabetes. J Theor Biol. 2000;206(4):605-19.
24. Topp BG, Atkinson LL, Finegood DT. Dynamics of insulin sensitivity, -cell function, and -cell mass during the development of diabetes in fa/fa rats. Am J Physiol Endocrinol Metab. 2007;293(6):E1730-5.
25. Ribbing J, Hamren B, Svensson MK, Karlsson MO. A model for glucose, insulin, and beta-cell dynamics in subjects with insulin resistance and patients with type 2 diabetes. J Clin Pharmacol. 2010;50(8):861-72.
26. Bridgewater A, Huard B, Angelova M. Amplitude and frequency variation in nonlinear glucose dynamics with multiple delays via periodic perturbation. Journal of Nonlinear Science. 2020;30(3):737-66.
27. Sedaghat AR, Sherman A, Quon MJ. A mathematical model of metabolic insulin signaling pathways. American Journal of Physiology-Endocrinology and Metabolism. 2002;283(5):E1084-E101.
28. Mason IC, Qian J, Adler GK, Scheer F. Impact of circadian disruption on glucose metabolism: implications for type 2 diabetes. Diabetologia. 2020;63(3):462-72.
29. Kahn SE, Hull RL, Utzschneider KM. Mechanisms linking obesity to insulin resistance and type 2 diabetes. Nature. 2006;444(7121):840-6.
30. Forbes JM, Cooper ME. Mechanisms of diabetic complications. Physiological reviews. 2013;93(1):137-88.
31. Bloomgarden ZT. Developments in diabetes and insulin resistance. Diabetes Care. 2006;29(1):161-7.
32. Efendić S, Wajngot A, Cerasi E, Luft R. Insulin release, insulin sensitivity, and glucose intolerance. Proceedings of the National Academy of Sciences. 1980;77(12):7425-9.
33. Smith GI, Shankaran M, Yoshino M, Schweitzer GG, Chondronikola M, Beals JW, et al. Insulin resistance drives hepatic de novo lipogenesis in nonalcoholic fatty liver disease. The Journal of clinical investigation. 2020;130(3):1453-60.
34. Alves-Bezerra M, Cohen DE. Triglyceride Metabolism in the Liver. Compr Physiol. 2017;8(1):1-8.
35. Gad AI, Ibrahim NF, Almadani N, Mahfouz R, Nofal HA, El-Rafey DS, et al. Therapeutic Effects of Semaglutide on Nonalcoholic Fatty Liver Disease with Type 2 Diabetes Mellitus and Obesity: An Open-Label Controlled Trial. Diseases. 2024;12(8):186.

Applied Chemical Engineering (2024) Volume 7 Issue 3
doi: 10.59429/ace.v7i3.5563

Supplementary Material

Table 1. The equations describing the dynamics of the Insulin, Glucose, and FFA model

Number	Variable	Variable	Balance	Initial Conditions
1	the amount of insulin in the plasma	I_P	$\frac{dI_p}{dt} = f_1(G) - E(\frac{I_p}{V_p} - \frac{I_i}{V_i}) - \frac{I_p}{t_p}$	90.0 mmol/L
2	In addition, there are three variables	I_i	$\frac{dI_i}{dt} = E * (\frac{I_p}{V_p} - \frac{I_i}{V_i}) - \frac{I_i}{t_i}$	138 mmol/L
3	glucose in the plasma and intercellular space	G	$\frac{dG}{dt} = G_{in} - f_2(G) - f_3(G) * f_4(I_i) + f_5(x_3)$	13000 mmol/L
3(1)	glucose in the plasma and intercellular space	G	$\frac{dG}{dt} = G_{in} - f_2(G) - \frac{1}{5}f_3(G) * f_4(I_i) - \frac{4}{5}f_3(G) * f_4(I_i) + f_5(x_3)$	13000 mmol/L
4	represent the above-mentioned	X_1	$\frac{dx_1}{dt} = \frac{3}{t_d} * (I_p - x_1)$	70 mmol/L
5	delay between insulin in plasma and its effect on the hepatic glucose production	X_2	$\frac{dx_2}{dt} = \frac{3}{t_d} * (x_1 - x_2)$	70 mmol/L
6		X_3	$\frac{dx_3}{dt} = \frac{3}{t_d} * (x_2 - x_3)$	70 mmol/L
7	The pancreatic insulin production controlled by the glucose concentration	$f_1(G)$	$f_1(G) = \frac{R_m}{1 + \exp((C_1 - G/V_g)/a_1)}$	-
8	Insulin-independent glucose utilization (glucose uptake by the brain and nerve cells)	$f_2(G)$	$f_2(G) = U_b(1 - \exp(-G/(C_2 * V_g)))$	-
9	The glucose dependent term in the function describing glucose utilization is assumed to be which agrees with experimental result	$f_3(G)$	$f_3(G) = \frac{G}{C_3 * V_g}$	-
10	The insulin dependent term	$f_4(I_i)$	$f_4(I_i) = U_0 + \frac{U_m - U_0}{1 + \exp(-\beta \ln(I_i/C_4(1/V_i + 1/Et_i)))}$	-
11	The influence of insulin on the hepatic glucose production	$f_5(x_3)$	$f_5(x_3) = \frac{R_g}{1 + \exp(\alpha (x_3/V_p - C_5))}$	-
12	liver glucose	G_L	$\alpha_L \frac{dG_L}{dt} = S_G(t) - k_{gl}G_L + k_{gl2}G_B - \frac{v_{LG}G_L}{k_{LG} + G_L} - \frac{v_{LH}G_L}{k_{LH} + G_L}\left(\frac{1}{1 + k_{rep}P_L}\right) + k_{6I}P_L$	8 mmol/L
13	liver glycogen	Y_L	$\alpha_L \frac{dY_L}{dt} = \frac{1}{2}k_{yI}IP_L\left(1 + \tanh\left(\frac{I_{max} - Y_L}{C_0}\right)\right) - \frac{\beta_L}{1 + k_{dI}I}\left(\frac{Y_L}{Y_L + y_0}\right)$	50 mmol/l

Table 1. (*Continued*)

14	liver glucose-6-phospahte	P_L	$\alpha_L \frac{dP_L}{dt} = -\frac{1}{2}k_{yI}IP_L\left(1+\tanh\left(\frac{I_{max}-Y_L}{C_0}\right)\right)+\frac{\beta_L}{1+k_{dI}I}\left(\frac{Y_L}{Y_L+y_0}\right)+\frac{\beta_6 R_L}{1+k_{p6}I}+\frac{v_{LG}G_L}{k_{LG}+G_L}+\frac{v_{LH}G_L}{k_{LG}+G_L}\left(\frac{1}{1+k_{rep}P_L}\right)-k_P IP_L-k_{6I}P_L+k_{gp}L_A$	2.06 mmol/l
15	free fatty acids in liver	R_L	$\alpha_L \frac{dR_L}{dt} = k_{PP}R_M + k_p IP_L - \frac{\beta_6 R_L}{1+k_{P6}I} - k_{aI}IR_L + \mu_B$	0.37 mmol/L
16	triacylglycerol storage pool in liver	A_L	$\alpha_L \frac{dA_L}{dt} = 3k_{cI}T_{CB} + k_{bI}A_{NB} + 3k_r T_{LB} + k_{aI}IR_L + \frac{3v_{10}T_L}{k_{10}+T_L} + \frac{3v_6 A_L}{k_6+A_L} - \frac{3v_8 A_L}{k_8+A_L} - \frac{k_7 A_L}{1+k_5 I}$	0.57 mmol/L
17	TAG storage pool	T_L	$\frac{dT_L}{dt} = \frac{v_8 A_L}{k_8+A_L} - F(I)\frac{v_9 T_L}{k_9+T_L} - \frac{v_{10}T_L}{k_{10}+T_L}$	40 mmol/L
18	TAG secretary pool in liver	S_L	$\frac{dS_L}{dt} = \frac{3v_6 A_L}{k_6+A_L} - k_{9a}S_L$	0.0149 mmol/l

Table 2. List of dynamics of the Insulin, Glucose, and FFA model parameters [8, 9, 12, 13]

Number	name	value	Description
1	α_A	15.6L	adipose tissue volume
2	α_L	1.60 L	liver tissue volume
3	β_6	31.6L/min	rate of liver de novo lipogenesis from pyruvate
4	β_L	12L/min	liver glycogenolysis
5	μ_1	0.588 mmol/min	Plasma glucose usage
6	C_0	0.1mmol/L	small parameters
7	k_5	0.05/mmol	flux control coefficient for insulin inhibition of free fatty acid oxidation
8	k_{61}	4L/min	liver glucose dephosphorylation rate
9	k_6	0.3mmol/L	affinity for very low-density lipoprotein 2 triglyceride secretion through secretory pathway
10	k_7	0.759L/min	maximum rate of free fatty acid oxidation
11	k_8	0.625mmol/L	affinity for esterification of free fatty acids to triglycerides
12	k_9	43.583mmol/L	affinity of additional bulk lipidation
13	k_{9a}	1L/min	release of very low-density lipoproteins from secretory pathway
14	k_{10}	0.625mmol/L	affinity for hydrolysis of triglycerides to secretory pool
15	k_{12}	0.2	increased fraction of very low-density lipoprotein 1 secretion by insulin
16	k_{13}	15mmol/L	rate at which insulin modifies the fraction of very low-density lipoprotein 1 to very low-density lipoprotein 2 secretion
17	k_{14}	0.6	basal very low-density lipoprotein 1 secretion fraction

Table 2. (*Continued*)

18	k_{22}	48mmol/min	excess insulin secretion rate due to glucose stimulation
19	k_{al}	0.00002L^2/mmol min	pyruvate to acetyl coenzyme A conversion rate
20	k_{ba}	0.0104L/min	adipose uptake of endogenous lipoprotein triglycerides
21	k_{bl}	0.156L/min	liver uptake of plasma non-esterified fatty acids
22	k_{cl}	0.0075L/min	liver free fatty acid uptake of chylomicron triglycerides
23	k_d	1.733×10^8L/mmol	insulin degradation rate
24	k_{dl}	3.5×10^8mmol/L	liver glycogenolysis; insulin-inhibited rate
25	k_{gp}	0.311L/min	glucose-6-phospahte uptake from adipose glycerol
26	k_{LG}	0.0115mmol/L	Michaelis–Menten constant of glucokinase in liver
27	k_{LH}	0.0115mmol/L	Michaelis–Menten constant of glucokinase in liver
28	k_P	1.41×10^7mmol/L	rate of insulin-mediated glucose-6-phoshate to pyruvate
29	k_{PP}	0.5	rate of muscle pyruvate transport to liver
30	k_{p6}	$1.93\times10^8L^2$/mmol min	constant of pyruvate conversion to glucose-6-phospate
31	k_{yl}	1.28×10^6 L^2mmol^{-1} min^{-1}	rate of the glycogen synthesis stimulated by insulin
32	k_r	0.00058mmol	rate of endogenously derived lipoprotein triglycerides by liver as free fatty acids
33	k_{rep}	2.98mmol/L	glucose-6-phospahte inhibition constant of hexokinase in muscle
34	k_t	0.00348mmol/L	uptake rate of plasma endogenous triglycerides into muscle free fatty acids
35	l_{max}	400mmol	maximum glycogen store of liver
36	v_6	0.6mmol/L	rate of glycogen transport
37	v_8	0.333mmol/min	rate of glycogen transport
38	v_9	0.6mmol/L	rate of triglyceride release into plasma
39	v_{10}	0.1mmol/min	rate of triglyceride storage conversion to free fatty acids
40	v_{12}	40mmol L^{-1}	constant in triglyceride release into plasma
41	v_{LG}	14.3mmol/min	maximum rate of glucokinase in liver
42	v_{LH}	5.57mmol/min	maximum rate of hexokinase in liver
43	y_0	0.1mmol/min	range of liver glycogen concentration over which the release drops to zero)
44	V_p	3L	the distribution volume for insulin in plasma
45	V_i	11L	the effective volume of the intercellular space
46	V_g	10L	-

Table 2. (*Continued*)

47	E	0.2L min^{-1}	transfer rate E between insulin between plasma and intercellular space
48	t_p	6L min	Insulin degradation is assumed to be exponential , with time constant tp for insulin in plasma
49	t_i	100 L min	Insulin degradation is assumed to be exponential , with time constant t_i for insulin in the intercellular space
50	t_d	36 L min	This delay is assumed to be of third order with a total time td
51	R_m	210 mU min^{-1}	-
52	a_1	300 mg L^{-1}	-
53	C_1	2000 mg L^{-1}	-
54	U_b	72 mg min^{-1}	-
55	C_2	144 mg L^{-1}	-
56	C3	1000 mg L^{-1}	-
57	U_0	40 mg min^{-1}	-
58	U_m（	940 mg min^{-1}	-
59	β	1.77	-
60	C_4	80 mU I^{-1}	-
61	R_g	180 mg min^{-1}	-
62	α	0.29mU I^{-1}	-
63	C_5	26 mU I^{-1}	-
64	Gin	216mg min^{-1}	glucose is supplied to the plasma at an exogenously controlled rate

The above glucose-insulin model is based on the mathematical model of blood glucose balance established by Tolic and Sturis team in 2000, and we have made the following adjustments:

The links of glucose generation and glycogen synthesis in the liver were re-established, and gluconeogenesis and glycolysis occurred in the liver. For the sake of simplification of the model, only the links of glucose conversion into glycogen in the liver were concerned, and other links were ignored. Moreover, according to the study[10], the conversion ratio of glycogen to grape in the liver was 80%, that is, the proportion of glucose consumption accounted for 20%, so the equation 3 was changed to 3(1).

$$\frac{dG}{dt} = G_{in} - f_2(G) - \frac{1}{5}f_3(G) * f_4(I_i) - \frac{4}{5}f_3(G) * f_4(I_i) + f_5(x_3)$$

$\frac{1}{5}f_3(G) * f_4(I_i)$ represents the part of glucose that is used in response to insulin,$\frac{4}{5}f_3(G) * f_4(I_i)$ represents the part of the liver where glucose is converted into glycogen. Considering that the part of glucose absorption includes the part of food digestion and absorption, and the glucose converted by food digestion and absorption as set in the paper, we set 125 mg min^{-1}, and the glucose infusion rate of G_{in} in the previous equation was 216mg min^{-1}, G_{in} was split into two parts. One portion represents 125 mg min^{-1} for food digestion and absorption, and the other 95mg min^{-1} represents intravenous infusion of partial glucose.